

Strong Coupling Effects with Quantum Metamaterials.

Jonathan Plumridge, Edmund Clarke, Ray Murray and Chris Phillips, *Experimental Solid State Group, Physics Department, Imperial College, Prince Consort Road London SW7 2AZ, UK.*

Abstract

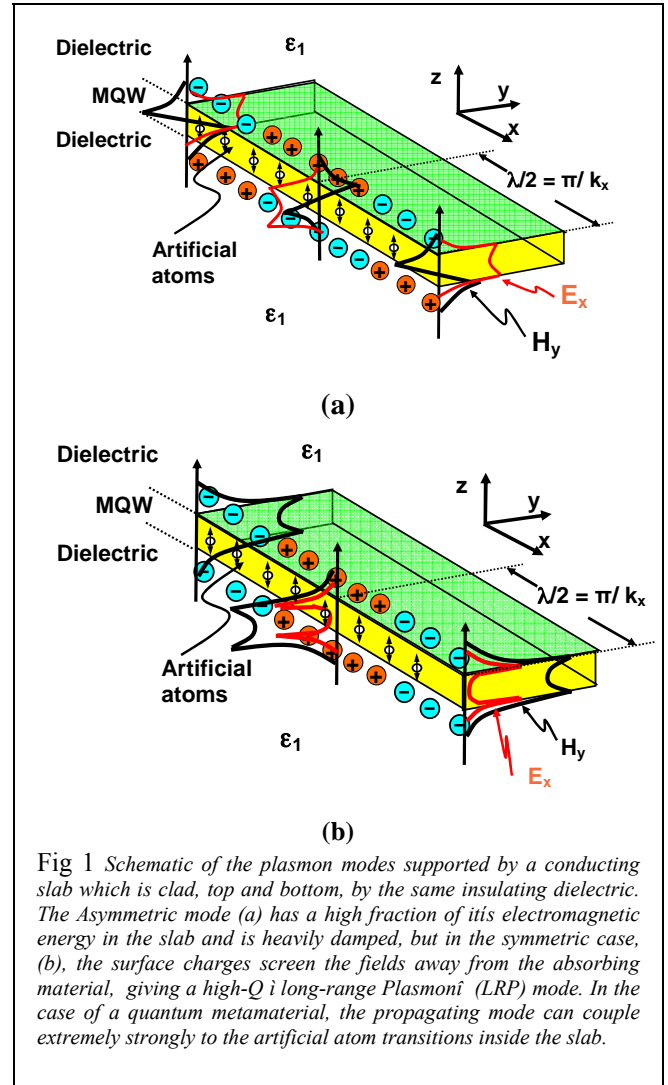
Plasmons are collective excitations¹ of groups of mobile electrons. In small metal structures they generate enormously enhanced electric fields, which are resonant and geometry-sensitive. They have led to a host of ‘Plasmonic’ applications², in sensing, biophotonics³ and metal optics⁴, and they are harnessed in so-called metamaterials, where artificially structuring a metal, on a sub-wavelength length scale, produces designable optical properties which are unlike any found in nature⁵.

Here we use semiconductor technology to make a new quantum metamaterial. It has the optical characteristics of a metal in two directions, but behaves like a collection of artificial atoms, whose properties can be designed-in using quantum theory, in the third. We find that this new quantum metamaterial supports a new type of guided plasmon.

In the ‘Strong-coupling’ (SC) regime two excitations are more strongly coupled to each other than to the rest of the Universe, allowing the transfer of quantum information between them. SC is a pre-requisite for quantum-computers and for the observation of second quantisation effects^{6,7}. Here we also show how the plasmon, and the artificial atom transitions can be made degenerate, and that the strong-coupling regime can be readily accessed.

This quantum metamaterial also allows the propagating Plasmon to be excited and probed optically, and the strong-coupling can be controlled with a small externally applied voltage⁸, so a single Plasmon excitation could be made to interact with a separate groups of artificial atoms as it is guided through a patterned device. Consequently this development has transformed the field of Plasmonics from the realm of passive devices and interconnects to an active technology which promises a new range of compact and coherent opto-electronic circuits, switches and devices.

Surface-plasmon-polaritons (SPPs) have long been known to be supported at the planar boundary between two materials whose dielectric constants are opposite in sign, and their strongly enhanced fields have proven valuable for the realisation of subwavelength optics⁴, non-linear optics², optical sensors³, and mid-IR diode laser cavities⁹.



Normally the negative dielectric is a strongly absorbing metal. This usually leads to heavily damped modes which propagate for $< 100 \mu\text{m}$ ^{1,2}, but recently it has been shown that sufficiently thin metal slabs can support guided plasmon modes which propagate many millimetres¹⁰. As the slab thickness is reduced, the SPP modes at its two faces start to couple together. The coupling produces two new modes which, if the cladding is the same above and below, are exactly symmetric and antisymmetric. The antisymmetric mode still has most of its electromagnetic

energy in the slab (fig. 1(a)) and will be heavily damped, but the symmetric one has its energy is screened out of the slab (fig.1 (b)), and this gives a lightly damped Long Range Plasmon (LRP) mode which propagates long distances. This LRP mode has the curious property that it is supported only in the presence of strong absorption in the central slab; the stronger the absorption, the narrower the LRP resonance and the further it can propagate¹⁰.

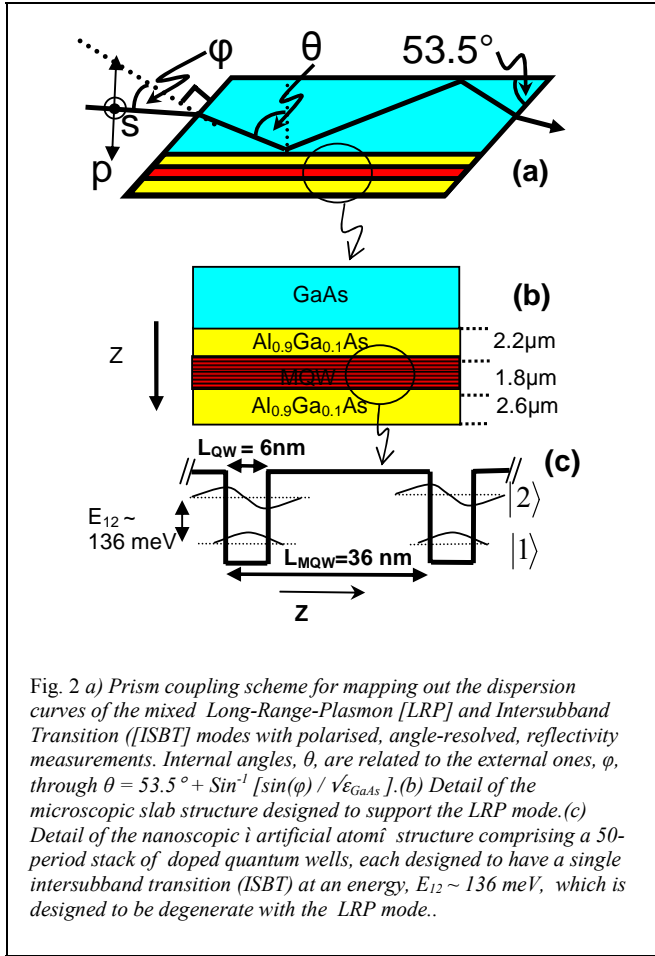
determined by the doping density, and its energy, which corresponds to the intersubband transition (ISBT) between the confined electron states, can be independently tailored, by the nanostructure design to match that of the LRP (Fig.2).

Demonstrations of Strong-coupling (SC) typically involve a dipole-allowed electronic transition coupled to the photon modes of a small optical cavity^{11,12}. If the two oscillators are sufficiently localised in energy (i.e. a sharp transition line coupled to a high finesse cavity) and space (i.e. a small optical mode volume) their Vacuum Rabi coupling energy, $\hbar\Omega_{VR}$, may exceed the linewidths of both the electronic transition and the cavity resonance. Tuning the modes' energies through degeneracy now generates anticrossing behaviour and mixed light-matter modes¹³. Exotic Photon statistical effects also appear which can be explained only with theories in which both the electron and photon fields are fully quantised^{6,7}. Here we study anticrossing behaviour to show that the SC regime can be realised in a robust and manufacturable solid-state system, even though the excitation linewidths are large by the standards of previous SC experiments.

The multiple-quantum-well (MQW) sample is grown by molecular-beam-epitaxy and comprises 50 periods, each with a 6nm wide GaAs QW separated by a 30 nm $\text{Al}_{0.35}\text{Ga}_{0.65}\text{As}$ barrier. The n-doping ($n_s \sim 6.5 \times 10^{11} \text{ cm}^{-2}$ per well) populates only the lowest confined QW state, giving a single intersubband-transition¹⁴ (ISBT) over the spectral range studied. Electrons in neighbouring wells are quantum-mechanically isolated, but they couple via by the Coulomb interaction. The MQW slab is clad above and below with the same undoped $\text{Al}_{0.9}\text{Ga}_{0.1}\text{As}$ material which is thick enough ($> 2\mu\text{m}$) to keep the LRP mode away from lossy parts of the structure, and thus closely approximate the dielectric symmetry assumed in the modelling.

The wafer was cut and polished into a rhombohedral prism (fig.2) for polarised, angle-resolved reflectivity spectra to be taken, at an angular resolution of $\varphi \sim 2.5^\circ$. Substrate absorption makes it impossible to get good quantitative s- and p- polarised spectra in this situation, but the ratio of s- to p- polarised reflectivity can be measured and calibrated with high confidence. S- and p- polarised features occur at different energies, so in practice this is not a serious limitation.

Tuning the internal angle of incidence, θ , to the slab, changes the in-plane wavevector $k_x = \underline{K} \sin(\theta) [\epsilon_{\text{GaAs}}]^{1/2}$. Here \underline{K} is the free-space wavevector of the beam outside the sample, and $\epsilon_{\text{GaAs}} = 10.36$ the dielectric constant of the GaAs substrate¹⁵. This scans through the LRP dispersion curve, and allows the two excitations to be tuned through degeneracy.



Our experiments use semiconductors. Their mature fabrication technology lets us structure samples microscopically, to support analogues of the metallic LRP modes. However, we can also structure them on a nanoscopic scale, which is both small ($< 1/100$ of a wavelength) enough to be invisible to the plasmon electromagnetic fields, and small enough to modify, through the rules of quantum mechanics, the behaviour of the electrons in the slab. The plasmon 'sees' a slab of quantum metamaterial; its electrons are free to move in the x-y slab plane, giving a metallic response to light polarised in that direction, but their z-motion is completely quantised by confining potential wells, so light sees a single Lorentzian oscillator. Its oscillator strength is

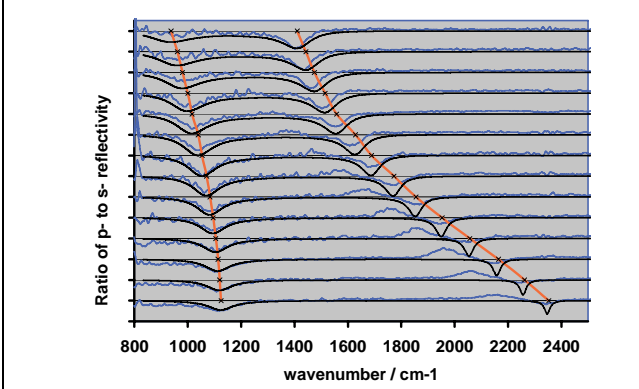


Fig.3 Angle resolved reflectivity spectra, spectra correspond to external angles ranging from $\phi = 61^\circ$ to $\phi = 35^\circ$ (highest trace), in 2° steps. with successive traces shifted vertically for clarity with the interval between successive traces corresponding to a 100% dip in reflectivity. Blue curves: experimental data, showing ISBT at 1100 cm^{-1} and the LRP, at $\sim 2300 \text{ cm}^{-1}$, before being brought into resonance, where they anticross with a coupling energy of $\sim 65 \text{ meV}$. Black curves, results of the transfer matrix reflectivity calculation for p-polarised light.

The measured spectra (Fig.3) each show two pronounced features, an ISBT-like excitation at $\sim 1100 \text{ cm}^{-1}$ / 136 meV , and a LRP like feature which angle tunes from $\sim 2400 \text{ cm}^{-1}$ / 297 meV to $\sim 1400 \text{ cm}^{-1}$ / 173 meV . The ISBT red shifts, by up to $\sim 200 \text{ cm}^{-1}$ / 24 meV , as the LRP energy is tuned towards it, and clear anti-crossing behaviour appears, with an anticrossing energy, $\hbar\omega_{\text{VR}} \sim 65 \text{ meV}$, some 8 times larger than the linewidth of either excitation.

We model these curves with an optical transfer matrix (TM) method¹⁶, which is well suited to computing distributions of electric and magnetic fields and their Poynting vectors in planar multilayers. It also gives plane-wave reflectivity and transmission spectra as a function of angle, wavelength and polarisation. The sub-wavelength nature of the nanoscale structuring fully justifies an effective-medium approach¹⁷, and we write the MQWs optical response as a complex, anisotropic dielectric tensor

$$\bar{\epsilon}_2 = \begin{pmatrix} \epsilon_{xx} & 0 & 0 \\ 0 & \epsilon_{yy} & 0 \\ 0 & 0 & \epsilon_{zz} \end{pmatrix} \quad (1)$$

$$\frac{1}{\epsilon_{zz}} = \frac{1}{\epsilon_z} - \left(\frac{\omega_p^2 f_{12}}{2\omega\gamma_2 \epsilon_w} \right) \frac{1}{\frac{E_{12}^2 - \omega^2}{2\gamma_2 \omega} - i}. \quad (3)$$

Where ϵ_y and ϵ_z are the mean effective background dielectric constants, given by $\epsilon_y = (1 - L_{\text{qw}}/L_{\text{mqw}})\epsilon_b + (L_{\text{qw}}/L_{\text{mqw}})\epsilon_w$ and $\epsilon_z^{-1} = (1 - L_{\text{qw}}/L_{\text{mqw}})/\epsilon_b + (L_{\text{qw}}/L_{\text{mqw}})/\epsilon_w$,

where L_{qw} and L_{mqw} are the QW width and MQW period respectively, and $\epsilon_b(\epsilon_w)$ are the background dielectric constants corresponding to undoped barrier (well) materials.

The in-plane electrons response (eq.2) is modelled as a Drude free electron gas, characterised by a 2D plasma frequency $\omega_p = [n_s e^2 / m^* \epsilon_0 L_{\text{mqw}}]^\Omega$, where n_s is the areal electron density per well, m^* the electron effective mass and the other symbols have their usual meanings. The out of plane electrons response (eq.3) is that of a single ISBT artificial atom Lorentzian oscillator, at energy E_{12} , with an oscillator strength $f_{12} = 2m^* E_{12} |z_{12}|^2 / \hbar^2$. $z_{12} = \langle 1|z|2 \rangle$ is the intersubband dipole matrix element and γ_2 the electron scattering rate. Although each individual QW well is small compared with optical wavelengths [$L_{\text{mqw}} \ll 2\pi c (\epsilon_{zz})^{-1/2}$] the overall thickness, $d = N^* L_{\text{mqw}}$, of the slab containing N wells, need not be. We use $\epsilon_b = 9.88$ and $\epsilon_w = 10.36$ and $\epsilon_1 = 8.2$ for the dielectric constants of $\text{Al}_{0.35}\text{Ga}_{0.65}\text{As}$, GaAs and $\text{Al}_{0.9}\text{Ga}_{0.1}\text{As}$ respectively¹⁵.

We use $z_{12} = 2.05 \text{ nm}$ (from separate wave function calculations), $m^* = 0.067 m_0$ (where m_0 is the free electron mass) and $E_{12} = 136 \text{ meV}$. The ISBT linewidth, measured as 7.6 meV in a separate $\theta = 45^\circ$ absorption experiment, gives $\gamma_2 \sim 7.6 \times 10^{12} \text{ sec}^{-1}$, and in the absence of more detailed knowledge of the in-plane scattering mechanisms, we set $\gamma_1 = \gamma_2$. Running the model with these values, combined with the experimental sample parameters above, produces the theoretical p-polarised reflectivity curves of figure 3.

In terms of excitation energies and integrated absorption strengths the agreement between experiment and theory is excellent, and both generate anti-crossing energies ($\sim 65 \text{ meV}$) some ~ 8.5 times larger than the ISBT linewidths, i.e. well into the SC regime. At high angles of incidence the strong angle-dependence of the LRP energy means the measured LRP linewidths are limited by the $\phi \sim 2.5^\circ$ angular resolution. The broad positive excursions, just to the red of the highest energy LRP modes are due absorption from a heavily damped s-polarised mode, which is predicted by both the numerical model and an independent analytical treatment¹⁷.

It is the metallic character of the metamaterials in-plane optical response that supports the plasmon modes and generates the plasmonic field enhancement effects. If we examine the TM model closely we find regions where low-loss propagating modes are supported by the metamaterial slab even when the in-plane component of its response is the *same sign as the cladding*. This is unknown in metals, but possibly by virtue of the metamaterials extreme optical anisotropy¹⁷.

This same anisotropy is the reason why we can optically couple to modes which propagate so well. The in-plane metallicity allows for efficient optical coupling, but now this can be combined with damping (which is determined only by the z- component of the slab's response) which can be made very small. The result is a mode which can be coupled into with efficiencies of several tens of %¹⁷ and which propagates with 1/e distances > 100nm¹⁷. With the present, non-optimised sample the TM model predicts propagation distances of 2.1mm and 1.34 mm at photon energies (wavelengths) of 88meV (14µm) and 315 meV (3.94 µm) respectively.

By comparison with previous reports of SC between 2D electronic systems and planar microcavities, the vacuum-Rabi coupling energy can be written as¹¹

$$\hbar\Omega_{VR} = 2\hbar \left[\frac{e^2 N_{qw}}{2\epsilon_0 n_c^2 L_{eff} m_e} f_{ex} \right]^{1/2} \quad (4)$$

where N_{qw} is the number of layers in the stack, n_c their mean refractive index, $f_{ex} = n_s f_{12}$, is the oscillator strength per well per unit area, and L_{eff} is the effective length of the optical cavity with which the electrons are coupled. The other symbols have their usual meanings. We find that, using the dimensions of the experimental sample the TM model accurately reproduces the n_s^{Ω} splitting energy predicted by eq.4, and shows that $\hbar\Omega_{VR}$ values in excess of 90meV being possible at realistic doping levels of $n_s \sim 10^{12} \text{ cm}^{-2}$. These high values come from the shrinking of L_{eff} by the plasmonic compression of the mode volumes. ???JRP by what factor, to $L_{eff} = \text{WHAT}$, ROUGHLY????

In the future, refinements such as using high mobility modulation doped multilayers to support the LRP mode This could reduce the electron scattering rates, narrowing the LRP linewidth thus enhancing the degree of SC possible and further increasing the propagation distances.

The authors would like to thank Paul Stavrinou for stimulating discussions. Funding from the UK Engineering and Physical Sciences Research Council is gratefully acknowledged.

¹ H. Raether *Surface Plasmons on Smooth and Rough Surfaces and Gratings*, Springer Verlag, New York (1988)

² W. L. Barnes, A.Dereux and T. W. Ebbesen, **Nature** **424**, 824-830 (14 August 2003)

³ J Homola, **Anal. and Bioanalytical Chemistry**, **377**, (3) 528-539, (2003).

⁴ S. Kawata *Near-Field Optics and Surface Plasmon Polaritons*, Springer (2001)

⁵ D. R. Smith, J. B. Pendry, M. C. K. Wiltshire *Metamaterials and Negative Refractive Index* **Science** 6 August 2004: Vol. 305. no. 5685, pp. 788 - 792

⁶ E.T. Jaynes and F. W Cummings **Proc. IEEE**, **51** (1) 89-109 (1963).

⁷ M.O. Scully and M. S. Zubairy *Quantum Optics*, Cambridge University Press (1997).

⁸ M.M. Fejer, S.J.B.Yoo, R.L. Byer, A. Harwit and J.S.Harris, **Phys. Rev. Lett.** **62** (9), 1041-1044, (1989).

⁹ C. Sirtori et al **Opt.Lett.** **23** (1998) 1366, ; R. Kohler et al **Nature** **417**, 156, (2002).

¹⁰ J. C. Quail, J. G. Rako, and H. J. Simon, "Long-range surface-plasmon modes in silver and aluminum films," **Opt. Lett.** **8**, 377- (1983); F. Yang, J. R. Sambles, and G. W. Bradberry, **Phys. Rev. Lett.** **64**, 559-562 (1990).

¹¹ M S Skolnick, T A Fisher and D M Whittaker, **Semicond. Sci. Tech.**, **13**, 645-669 (1988).

¹² Reithmaier et al **Nature** **432** 197, (2004); Yoshie et al **Nature** **432**, 200, (2004)

¹³ D Dini, R K hler, A Tredicucci, G Biasio and Lucia Sorba *Microcavity polariton splitting of ISBT's* **Phys.Rev.Letts** **90**, (11) 116401, **March 2003** and E Dupont, H C Liu SR Schmidt and A Seilmeier, **Appl. Phys.Letts** **79** (26) 4925 (2001).

¹⁴ J F Dynes, M D Frogley, M Beck, J Faist and C C Phillips, **Phys. Rev Lett.** **94**, 157403 (2005).

¹⁵ C Palmer, P N Stavrinou, M Whitehead and C C Phillips. **Semicond.Sci. and Tech.** **17**, 1189-1192 (2002).

¹⁶ M. Zaluzny and C Nalewajko, **Phys. Rev. B**, **59** (20), 13043. (1999)

¹⁷ J R Plumridge and C C Phillips, **cond-matt/0701521**